

ELASTODYNAMIC STRESS INTENSITY FACTORS FOR
AN INTERFACE CRACK IN A LAYERED HALF SPACE

Huey-Ju Pearl Yang* and
David B. Bogy

Mechanical Engineering Department
University of California
Berkeley, CA 94720

INTRODUCTION

Many structures, both man-made and of natural origin, are composed of different elastic materials formed in layers. Often the layers are bonded together along common faces, but it can happen that the bonding is not perfect and flaws occur as cracks or regions of poor bonding in the interface. It is of importance to be able to detect these interface cracks, and one of the most practical methods for accomplishing this, in the cases of engineering interest, utilizes the scattering of elastic waves and the subsequent detection of these scattered waves by appropriate transducers. The goal of this work is to contribute to the theoretical basis for detecting the interface flaw by these means.

The method utilized here to solve the plane strain interface flaw problem is similar to that used by Neerhoff¹ for the antiplane problem. First we formulate the problem, where the elastic field is separated into the incident and scattered fields. The incident field is left arbitrary in the analysis until a particular choice is made later on for the purpose of obtaining numerical results. In Yang¹⁰ the Green's functions were derived for dilatational and rotational sources in the layer as well as the substrate. These Green's functions are used in conjunction with the appropriate form of Green's integral theorem, to reduce the problem to a system of singular integral equations. These integral equations are analyzed to determine the order of singularity in the stress field at the crack tip, and it is found that this singularity is of the oscillatory type, except for a certain class of composites. The methods of Muskhelishvili⁵ and Erdogan and Gupta⁶ are then utilized to reduce these singular integral equations to a system of algebraic equations suitable for numerical solution.

These equations are solved numerically for several sets of composites, and the results are presented in the form of Mode I and Mode II

*Currently with Earth Sciences Division, Lawrence Berkeley Laboratory, University of California, Berkeley, CA 94720.

stress intensity factors plotted as functions of dimensionless wave number for various ratios of layer depth to crack length.

THEORY

We consider the steady time-harmonic plane-strain problem for the cracked layered elastic half space shown in Fig. 1.

The time-reduced form of the displacement equations of motion for isotropic media is

$$(\lambda + \mu)\nabla\nabla\mathbf{u} + \mu\nabla^2\mathbf{u} + \rho\omega^2\mathbf{u} = -\rho\mathbf{f}. \quad (1)$$

The displacement and stress can be decomposed into the sum of incident and scattered parts according to

$$\mathbf{u} = \mathbf{u}^{(i)} + \mathbf{u}^{(s)}, \quad \boldsymbol{\tau} = \boldsymbol{\tau}^{(i)} + \boldsymbol{\tau}^{(s)}. \quad (2)$$

The solution of the scattered field problem formulated here is obtained in the following sections by a method of integral equations in a manner similar to that used for the corresponding anti-plane problem in Ref. [1]. This method utilizes Green's functions corresponding to point sources in the uncracked layered half space.

For this purpose we make use of Green's (divergence) theorem in the following form (for 3-D elasticity solution)

$$\iint_D (u_i^A \tau_{ij,j}^A) dA = \oint_{\partial D} (u_i^A \tau_{ij}^B - u_i^B \tau_{ij}^A) n_j ds, \quad (3)$$

where ∂D denotes the boundary of the finite region D that surrounds the crack and \mathbf{n} is the outward unit normal to ∂D . Letting $\mathbf{u}^A = \mathbf{u}^{(s)}$, $\mathbf{u}^B = \mathbf{u}_L$ and $\mathbf{u}^A = \mathbf{u}^{(s)}$, $\mathbf{u}^B = \mathbf{u}_T$, respectively, where $\mathbf{u}^{(s)}$ is the displacement of the scattered field and \mathbf{u}_L , \mathbf{u}_T denote the dilatational and rotational wave fields associated with the Green's functions, we can derive the potentials $\phi^{(s)}(\underline{X}_p)$, $\psi^{(s)}(\underline{X}_p)$ for the scattered field.

Then we can obtain the result:

$$\begin{aligned} \phi^{(s)}(\underline{X}_p) &= -\frac{1}{\mu k_T^2} \int_{-a}^a ([u_x^{(s)}] \tau_{zx}^L + [u_z^{(s)}] \tau_{zz}^L) dx, \quad 0 < z_p < d \\ &- \frac{1}{\mu k_T^2} \int_{-a}^a ([u_x^{(s)}] \tau_{zx}^L + [u_z^{(s)}] \tau_{zz}^L) dx, \quad d < z_p < \infty \\ \psi^{(s)}(\underline{X}_p) &= -\frac{1}{\mu k_T^2} \int_{-a}^a ([u_x^{(s)}] \tau_{zx}^T + [u_z^{(s)}] \tau_{zz}^T) dx, \quad 0 < z_p < d \\ &- \frac{1}{\mu k_T^2} \int_{-a}^a ([u_x^{(s)}] \tau_{zx}^T + [u_z^{(s)}] \tau_{zz}^T) dx, \quad d < z_p < \infty \end{aligned} \quad (4)$$

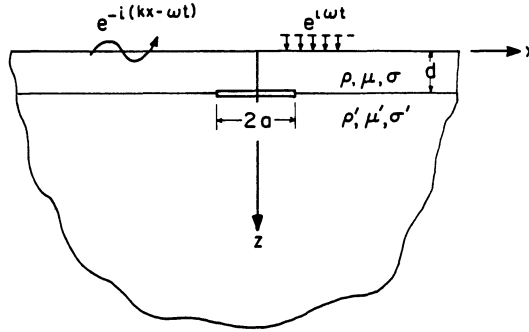


Fig. 1. Layered half space with interface crack and incident waves.

in which

$$\begin{aligned}
 [u_x(s)] &= \lim_{z \rightarrow d^+} u_x(s) - \lim_{z \rightarrow d^-} u_x^-(s) \\
 [u_z(s)] &= \lim_{z \rightarrow d^+} u_z(s) - \lim_{z \rightarrow d^-} u_z^-(s)
 \end{aligned}
 \tag{5}$$

and the integrals are taken along the crack and therefore the quantities τ_{zx}^L , etc. are evaluated along $z=d$.

Next we compute the interface tractions corresponding to the scattered wave potentials and impose the traction free conditions on the crack face to obtain integral equations for determining the unknown crack opening displacements and obtain the following pair of integral equations

$$\begin{aligned}
 &\int_{-a}^a \int_0^\infty \frac{p_1(k)}{\Delta(k)k} \sin[k(x-x_p)] dk] f_x(x) \\
 &- \int_0^\infty \frac{ip_2(k)}{\Delta(k)k} \cos[k(x-x_p)] dk] f_z(x) dx = \frac{\pi}{\mu\mu'} \tau_{zx}^{(i)}(x_p)
 \end{aligned}
 \tag{6}$$

$$\begin{aligned}
 &\int_{-a}^a \int_0^\infty \frac{ip_2(k)}{\Delta(k)k} \cos[k(x-x_p)] dk] f_x(x) \\
 &+ \int_0^\infty \frac{p_3(k)}{\Delta(k)k} \sin[k(x-x_p)] dk] f_z(x) dx = \frac{\pi}{\mu\mu'} \tau_{zz}^{(i)}(x_p), \quad -a < x_p < a
 \end{aligned}$$

where

$$f_x(x) = \frac{d}{dx} [u_x(s)(x)], \quad f_z(x) = \frac{d}{dx} [u_z(s)(x)]
 \tag{7}$$

and

$$\int_{-a}^a f_x(x) dx = 0, \quad \int_{-a}^a f_z(x) dx = 0.
 \tag{8}$$

The problem has therefore been reduced to the system of integral equations, which need to be solved for f_x and f_z for prescribed $\tau_{zx}^{(i)}$, $\tau_{zz}^{(i)}$, and subject to the resultant conditions above.

The integral equations we obtained appear to be of the first kind but the kernel functions contain infinite integrals which may have singularities. We know that the function $\Delta(k)$ has zeros corresponding to the propagating surface modes of the type studied in Ref. [3]. These roots may occur on or off the real k -axis and they determine poles in the complex k -plane of the integrands in the kernels. We must determine their locations for given geometry, material parameters, and frequency and take them into account in our numerical solution.

In addition to the zeros of $\Delta(k)$, we must investigate the behavior of the kernel integrands in the limit $k \rightarrow \infty$ and $k \rightarrow 0$. Also, the multi-valued functions γ_L , γ_T , γ'_L and γ'_T , defined as $\gamma_L^2 = k_L^2 - k^2$, etc., have branch points at $\pm k_L$, $\pm k_T$, $\pm k'_L$ and $\pm k'_T$, respectively. We choose the branches such that $\text{Re}(\gamma_L) > 0$, $\text{Re}(\gamma_T) > 0$ on the path of integration.

Making use of the asymptotic expressions to remove the singularities from the kernels, we obtain the following integral equations

$$\begin{aligned}
 & -\frac{\pi\delta_2}{\delta_0} f_z(x_p) + \frac{\delta_1}{\delta_0} \int_{-a}^a \frac{f_x(x)}{x-x_p} dx + \int_{-a}^a L(x_p, x) f_x(x) dx \\
 & -i \int_{-a}^a M(x_p, x) f_z(x) dx = \frac{\pi}{\mu\mu'} \tau_{zx}^{(i)}(x_p),
 \end{aligned} \tag{9}$$

$$\begin{aligned}
 & \frac{\pi\delta_2}{\delta_0} f_x(x_p) + \frac{\delta_1}{\delta_0} \int_{-a}^a \frac{f_x(x) dx}{x-x_p} + i \int_{-a}^a M(x_p, x) f_x(x) dx \\
 & -i \int_{-a}^a L^*(x_p, x) f_z(x) dx = \frac{\pi}{\mu\mu'} \tau_{zz}^{(i)}(x_p).
 \end{aligned}$$

The kernels $L(x_p, x)$, $M(x_p, x)$ are regular, which means that the system has only Cauchy singularities.

We next analyze the singular integral equations to determine the order of singularity in the solution functions $f_x(x)$ and $f_z(x)$. Here we follow the technique in Ref. [5] and define $F_x(x)$, $F_z(x)$ through

$$f_x(x) = F_x(x)/(a^2-x^2)^\alpha, \quad f_z(x) = F_z(x)/(a^2-x^2)^\alpha, \quad |x| < a \tag{10}$$

where $\text{Re}(\alpha) < 1$ and F_x, F_z are Holder continuous. Using the result

$$\phi(x_p) = \frac{1}{\pi} \int_{-a}^a \frac{f_x(x)}{x-x_p} dx = \frac{F_x(-a)\cot(\pi\alpha)}{(2a)^\alpha(a+x_p)^\alpha} - \frac{F_x(a)\cot(\pi\alpha)}{(2a)^\alpha(a-x_p)^\alpha} \tag{11}$$

together with a similar result for $f_z(x)$, and Eq. (4.11), we obtain, by analyzing the dominant part and taking the limit $x_p \rightarrow a$ (or $x_p \rightarrow -a$),

$$\begin{aligned}
 & \delta_1 F_x(a)\cot(\pi\alpha) + \delta_2 F_z(a) = 0 \\
 & \delta_2 F_x(a) - \delta_1 F_z(a)\cot(\pi\alpha) = 0.
 \end{aligned} \tag{12}$$

This system requires, for a nontrivial solution,

$$\left(\frac{\delta_2}{\delta_1}\right)^2 \sin^2(\pi\alpha) + \cos^2(\pi\alpha) = 0, \tag{13}$$

which is the same as the equation that determines the stress singularity at the tip of an interface crack in static problems (see Ref. [7]). In fact, it can be shown that (for plane strain)

$$\frac{\delta_2}{\delta_1} = \beta = \frac{\mu'(1-2\sigma) - \mu(1-2\sigma')}{2\mu'(1-\sigma) + 2\mu(1-\sigma')} \tag{14}$$

which is one of the composite parameters introduced in Ref. [8].

The solution for α is

$$\alpha = \frac{1}{2} \pm \frac{i}{\pi} \tanh^{-1}(\beta) = \frac{1}{2} + \frac{i}{2\pi} \ln \left(\frac{1+\beta}{1-\beta}\right). \tag{15}$$

Therefore, the well-known oscillating singularity occurs in the solution of the integral equations, unless $\beta=0$. If $\beta=0$, the crack tip singularity is $1/2$, as in the case of a homogeneous material. We will restrict our numerical solution of the integral equations to this case.

We now approximate the system of integral equations by a corresponding set of algebraic equations by first introducing dimensionless variables then decomposing the problem into its physically symmetric and anti-symmetric parts with respect to x . Next we recall the approximation formulas from Erdogan and Gupta⁶, when the functions $f_x(x)$, $f_z(x)$ appear in integrals with Cauchy kernels or with regular kernels. For functions appearing outside of integrals we use Lagrange interpolation polynomials together with the symmetries. Then we replace the integral equations with their algebraic approximation, which provides two complex $(n \times n)$ linear algebraic systems for determining the $2n$ complex unknown $F_x^S(\eta_i)$, $F_x^A(\eta_i)$, $F_z^S(\eta_i)$, $F_z^A(\eta_i)$, $i = 1, 2, \dots, n/2$.

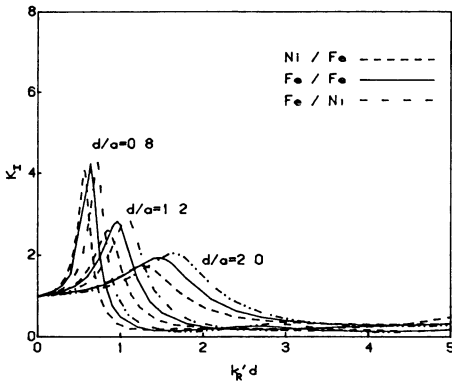


Fig. 2a. Mode I stress intensity factor for different combinations of materials = layer/substrate.

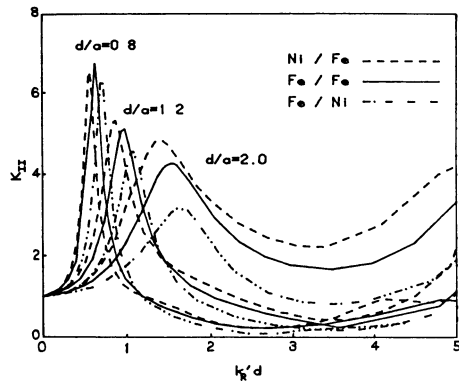


Fig. 2b. Mode II stress intensity factor correspondence with Fig. 2a.

We are now ready to solve numerically the system except for the singularity in the integrands of the integrals. These singularities are poles that occur in the complex k -plane at the zeros of $\Delta(k)$. It was shown by Farnell and Adler³ that in the "loading" case, for which the shear wave velocity of the layer is less than that of the substrate, only one Rayleigh-type pole occurs, and it is on the real k -axis. However, for the "stiffening" case, for which the substrate shear wave velocity is greater, more than one such pole may occur, depending on the frequency. In both cases, it is found (see Bogy and Gracewski⁴), that the poles never occur in the fourth quadrant ($\text{Re}(k) > 0, \text{Im}(k) < 0$) of the k -plane.

Two different ways have been used by others for dealing with these poles. Kundu and Mal⁹ use a technique of removing the singularities from the integrands. The other technique, used by Neerhoff¹ and Keer et al.², merely deforms the contour of integration below the real k -axis so that no poles occur on the path of integration. We chose the later method in this work.

NUMERICAL RESULTS

Various numerical results can be obtained from our analysis. We shall restrict the presentation here to the dynamic stress intensity factors K_I and K_{II} , at the crack tips, due to an incident wave resulting from a harmonic uniform normal traction applied at the boundary $z=0$.

Numerical calculations were carried out for three different material pairs: nickel/iron, aluminum/zinc, and nickel/gold. Both materials were considered as layer and substrate in each case. The material parameters were slightly adjusted in each case in order to satisfy the condition $\beta=0$. The actual values for the material parameters used are given in Ref. [10].

Figures 2a and 2b, respectively, show K_I , and K_{II} versus $k_R d$ for various ratios of layer thickness d to crack half length for three sets of material combinations. One set is for a nickel layer with iron substrate, one set is for iron layer with iron substrate, and the third set is for an iron layer on a nickel substrate. The material parameters for these two

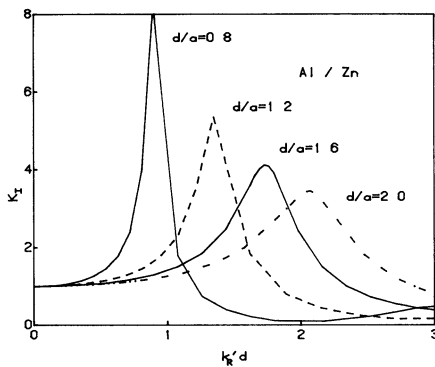


Fig. 3a. Mode I stress intensity factor for Al/Zn.

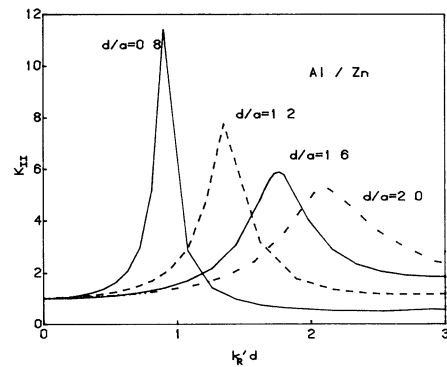


Fig. 3b. Mode II stress intensity factor for Al/Zn.

materials are not very different and the computations for this case caused less difficulties than for other cases in which the materials are radically different.

Figures 3a,b show K_I and K_{II} , respectively, as functions of $k_R d$ for various values of d/a for the case of an aluminum layer on a zinc substrate. Figures 4a,b show the corresponding results for a zinc layer on an aluminum substrate.

Finally, Figures 5a,b show K_I and K_{II} , respectively, as functions of $k_R d$ for various values of d/a for the case of a nickel layer on a gold substrate. Figures 6a,b show the corresponding results for a gold layer on a nickel substrate. This pair of materials had the greatest mismatch of material parameters of the three pairs considered.

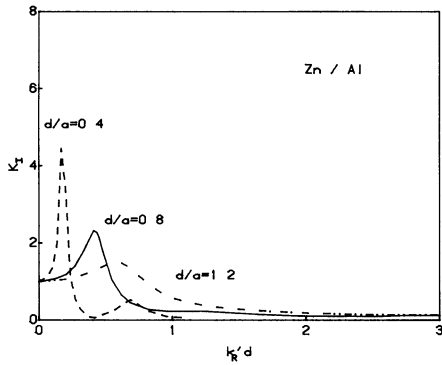


Fig. 4a. Mode I stress intensity factor for Zn/Al.

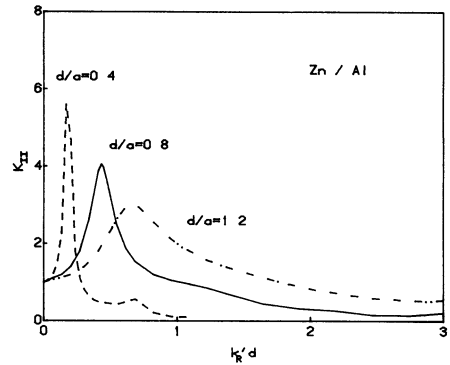


Fig. 4b. Mode II stress intensity factor for Zn/Al.

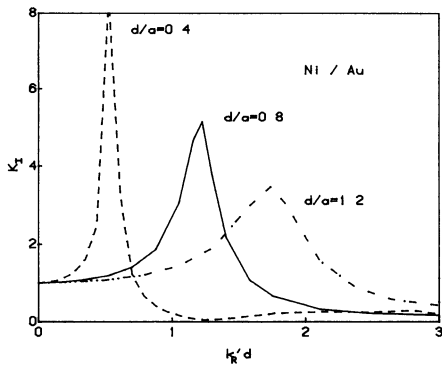


Fig. 5a. Mode I stress intensity factor for Ni/Au.

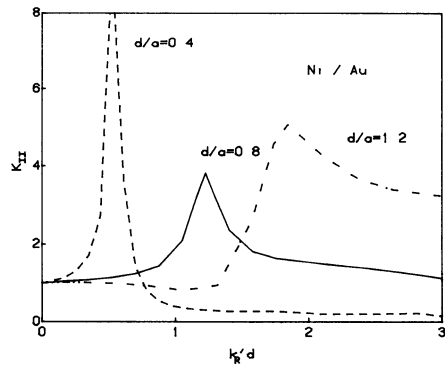


Fig. 5b. Mode II stress intensity factor for Ni/Au.

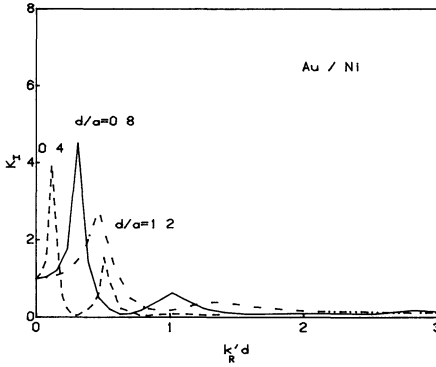


Fig. 6a. Mode I stress intensity factor for Au/Ni.

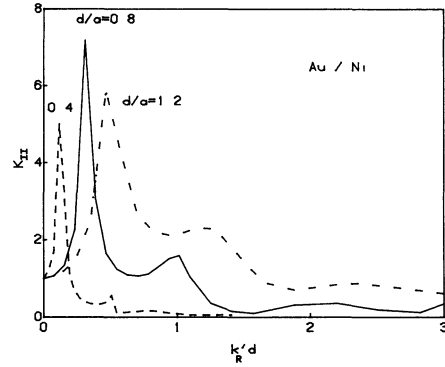


Fig. 6b. Mode II stress intensity factor for Au/Ni.

REFERENCES

1. F. L. Neerhoff, Diffraction of Love waves by a stress-free crack of finite width in the plane interface of a layered composite, Applied Scientific Research 35:265-315 (1979).
2. L. M. Keer, W. Lin, and J. D. Achenbach, Resonance effects for a crack near a free surface, J. Appl. Mech., to appear.
3. G. W. Farnell and E.L. Adler, Elastic wave propagation in thin layers, in: "Physical Acoustics," Academic, New York 9:35-127 (1972).
4. D. B. Bogoy and S. M. Gracewski, On the plane-wave reflection coefficient and nonspecular reflection of bounded beams for layered half-spaces underwater, J. Acoust. Soc. Am. 74:591-599 (1983).
5. N. I. Muskhelishvili, "Singular Integral Equations," Noordhoff Int. Publ. (1977).
6. F. Erdogan and G. D. Gupta, On the numerical solution of singular integral equations, Quart. Appl. Math. 30:525-534 (1972).
7. D. B. Bogoy, Two edge-bonded elastic wedges of different materials and wedge angles under surface tractions, J. Appl. Mech. 38:377-386 (1971).
8. J. Dundurs, Discussion, J. Appl. Mech. 36:650 (1969).
9. T. Kundu and A. K. Mal, Calculation of the surface response of a layered solid to a point dislocation source, private communication.
10. H.-J. P. Yang, Elastic wave scattering from an interface crack in a layered half space, Ph.D. Dissertation (1984).